Review Article

Mechanical behavior of polymer-based *vs*. metallic-based bioresorbable stents

Hui Ying Ang[1], Ying Ying Huang[2], Soo Teik Lim[1,3], Philip Wong[1,3], Michael Joner[4], Nicolas Foin[1]

[1]National Heart Centre Singapore, Singapore, Singapore; [2]School of Materials Science and Engineering, Nanyang Technological University, Singapore, Singapore; [3]Duke-NUS Medical School, Singapore, Singapore; [4]Deutsches Herzzentrum München, Technische Universität München, Munich, Germany

Contributions: (I) Conception and design: N Foin, HY Ang; (II) Administrative support: N Foin, HY Ang; (III) Provision of study materials or patients: All authors; (IV) Collection and assembly of data: N Foin, HY Ang; (V) Data analysis and interpretation: All authors; (VI) Manuscript writing: All authors; (VII) Final approval of manuscript: All authors.

Correspondence to: Dr. Nicolas Foin, MSc, PhD. National Heart Research Institute Singapore, National Heart Centre Singapore, 5 Hospital Drive, Singapore 169609, Singapore. Email: nicolas.foin@gmail.com.

Abstract: Bioresorbable scaffolds (BRS) were developed to overcome the drawbacks of current metallic drug-eluting stents (DES), such as late in-stent restenosis and caging of the vessel permanently. The concept of the BRS is to provide transient support to the vessel during healing before being degraded and resorbed by the body, freeing the vessel and restoring vasomotion. The mechanical properties of the BRS are influenced by the choice of the material and processing methods. Due to insufficient radial strength of the bioresorbable material, BRS often required large strut profile as compared to conventional metallic DES. Having thick struts will in turn affect the deliverability of the device and may cause flow disturbance, thereby increasing the incidence of acute thrombotic events. Currently, the bioresorbable poly-l-lactic acid (PLLA) polymer and magnesium (Mg) alloys are being investigated as materials in BRS technologies. The bioresorption process, mechanical properties, *in vitro* observations and clinical outcomes of PLLA-based and Mg-based BRS will be examined in this review.

Keywords: Bioresorbable stents; coronary artery disease; coronary stents; bioresorbable scaffolds (BRS); magnesium (Mg) stents; bioresorbable vascular scaffold (BVS)

Submitted Apr 12, 2017. Accepted for publication May 18, 2017.
doi: 10.21037/jtd.2017.06.30
View this article at: http://dx.doi.org/10.21037/jtd.2017.06.30

Introduction

Current metallic drug-eluting stents (DES) have thin struts and adopt biocompatible or biodegradable polymer coating which improved their safety profile, making them the device of first choice for the treatment of coronary artery disease (1). However, permanent caging of the vessel with a metallic implant runs the risk of impairing endothelial function, decreasing positive lumen remodeling, and the risk of side branches occlusion due to neointimal hyperplasia (2-6). In recent years, clinical observations from several large-scale DES registries have revealed the occurrence of late adverse events such as very late stent thrombosis or late target lesion revascularization (TLR) beyond 1 year, raising safety concerns of the device (7).

Hence, the concept of using bioresorbable scaffolds/stents (BRS) is an attractive strategy and has been credited as the fourth revolution in interventional cardiology. The BRS is expected to provide the necessary temporal support to the vessel and disappear in due time, allowing the vessel to return to a more natural and healed state (8). Theoretically, after the healing period, the BRS will degrade and be resorbed completely, leaving the vessel with a healthy endothelium, normal vasomotion and free of caging (9,10). The absence of any residual foreign material and restoration of endothelial coverage

Table 1 Mechanical and physical characteristics of bioresorbable scaffold and metallic stent materials. Adapted from (18-20)

Polymer	Tg (℃)	Tm (℃)	Modulus (GPa)	Strength (MPa)	Elongation at break (%)	Degradation (months)
PLA	60	180–190	2–4	65	2–6	18–30
PDLLA	55	Amorph	1–3.5	40	1–2	3–4
PLLA	60–65	175	2–4	60–70	2–6	>24
PGA	35–40	225–230	6–7	90–110	1–2	4–6
PDLGA (50/50)	45	Amorph	1–4.3	45	1–4	1–2
PLGA (82/12)	50	135–145	3.3–3.5	65	2–6	12–18
PCL	-54	55–60	0.34–0.36	23	>4,000	24–36
PLA/PCL (70/30)	20	100–125	0.02–0.04	2–4.5	>100	12–24
PC	~147	225	2–2.4	55–75	80–150	>14
WE43 (Mg alloy)	N/A	540–640	40–50	220–330	2–20	3–12
SS 316L	N/A	1,371–1,399	193	668	40	Biostable
Co-Cr	N/A	~1,454	210	235	40	Biostable

PLA, polylactic acid; PDLLA, poly-DL-lactic acid; PLLA, poly-L-lactic acid; PDLGA, poly-DL-lactide-co-glycolide; PGA, polyglycolide; PLGA, poly-lactic-co-glycolide; PCL, polycaprolactone; PLA/PCL, polylactic acid/polycaprolactone; Mg, magnesium; SS, stainless steel; Co-Cr, cobalt chromium.

would also reduce the risk of late stent thrombosis and the requirement for long-term dual antiplatelet therapy (DAPT) theoretically (11-13).

Majority of the materials used in the fabrication of BRS are biodegradable polymers such as poly-L-lactic acid (PLLA) while bio-corrodible metals such as magnesium (Mg) and iron are also employed (14). Polyesters are the main polymers used in BRS technologies due to their tailorable biodegradability and unprocessed polyesters such as PLLA will typically have a tensile modulus that is approximately 100-fold lower than cobalt or stainless steel material. As the tensile modulus is directly related to the resulting radial strength, scaffolds fabricated from these bioresorbable materials may require up to 240% thicker struts to match up with the current DES (15). Mg can be alloyed with one or more elements (rare earth metals, aluminium, zinc etc.) to form a class of bioresorbable material known as biocorrodible metals. Mg alloys have enhanced mechanical properties that allows the Mg BRS to have potentially good radial strength compared to conventional polymer based BRS (9,16). In theory, bioresorbable stents made from biocorrodible metals are able to have thinner struts and lower profile compared to polymeric scaffolds (17). A summary of the mechanical and physical properties of different bioresorbable materials used in the fabrication of BRS and DES are shown in *Table 1* for comparison. In this review, the mechanical behavior of current polymer-based and metallic-based BRS will be explored and discussed.

Polymer-based BRS

Polymers such as PLLA, poly-DL-lactic acid (PDLLA), poly(lactide-co-glycolide) (PLGA), polycaprolactone (PCL) and polycarbonates (PC) have been explored as potential material for BRS platforms. Although polyglycolide (PGA) has higher strength and stiffness than PLLA, the low ductility and difficulty in processing the material makes it unsuitable for BRS fabrication. PLGA is fabricated from the random copolymerization of PLA and PGA to prolong PGA's degradation. The inclusion of PLA adds methyl groups that increase its hydrophobicity, hence altering its degradation rate (21,22). PCL is a semi-crystalline polymer with higher flexibility than PLLA but significantly lower tensile modulus and strength due to lower crystallinity. As seen in *Table 1*, PLLA has comparatively higher tensile strength and modulus than PDLA and PCL and a slower absorption time than PLGA. This makes PLLA the most commonly used polymeric candidate for BRS fabrication. The additional methyl group in PLLA causes the polymer to be more hydrophobic and stable against hydrolysis as compared to PGA (22). Furthermore, PLLA

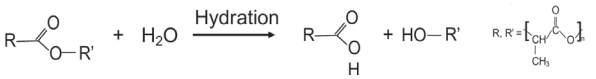

Figure 1 Reaction pathway for hydrolytic degradation of PLLA. PLLA, poly-l-lactic acid.

is biocompatible, biologically inert and has been used widely in biomedical application such as sutures and tissue engineering scaffolds.

Some PLLA-based BRS include: ABSORB bioresorbable vascular scaffold (BVS) (Abbott Vascular), DESolve (Elixir Medical), FORTITUDE/APTITUDE (Amaranth), ArterioSorb (Arterius), MIRAGE (Manli Cardiology), MeRes100 (Meril Life Sciences). Reva Medical's FANTOM BRS on the other hand is fabricated from tyrosine derived PC which is a group of homologous carbonate-amid copolymers with differing length of their respective alkyl ester pendent chains.

Mechanical properties of polymer-based BRS

Bioresorption behavior of PLLA

PLLA, a semicrystalline polymer (maximum crystallinity =70%) with the highest glass transition temperature, Tg, has relatively high tensile properties among the general biodegradable polymers (23). The Tg of a polymer is the temperature at which the reversible transition in amorphous regions within a semicrystalline polymer from a hard and relatively brittle state into a viscous or rubbery state occurs. However, unprocessed PLLA has mechanical strength that is still significantly lower as compared to the metals used conventionally in DES fabrication. PLLA devices have also limit of expansion and can fracture due to over-dilation. Thus, it is important to improve the expandability of the BRS while maintaining radial strength (24). Therefore, material processing and stent design modifications are needed to achieve a good acute performance of the BRS.

The degradation and subsequent absorption of PLLA takes place in three stages via hydrolysis, which affects the polymeric device's mechanical performance. The hydrolysis process is a bimolecular nucleophilic substitution reaction catalyzed by the presence of either acids or bases and a polymer chain scission event usually takes place at an ester bond as seen in *Figure 1*.

In the first stage, hydrolysis of the amorphous polymer tie chains occurs and the molecular weight decreases with little effect on mechanical performance. The amorphous segments are less packed and more susceptible to hydrolysis due to the hydrophilic carboxylic acid end group, causing a slight reduction in crystallinity (25). In the second stage, the device experiences a decrease in mechanical strength due to scission of the amorphous tie chains linking crystalline regions. At this stage, the polymer fragments into low-weight oligomers and mass loss, cracks and structural discontinuities will be observed (25). Lastly, the monomer (e.g., L-lactate) is transformed into pyruvate, which enters the Krebs cycle and is converted into carbon dioxide and water. The end products are subsequently excreted from the body through the kidneys or lungs, completing the bioresorption of the polymer (26,27).

In vitro observations

Mechanical properties

Abbott Vascular's Everolimus-eluting ABSORB BVS is the first BRS to achieve the FDA's approval and is the most widely examined PLLA-BRS in the market presently. Despite extensive differences between the intrinsic properties of PLLA and metallic alloys, bench testing revealed comparable radial strength and similar recoil between the BVS and DES when standard measurement methods were used. The review published by Oberhauser *et al.* reported that the ABSORB BVS had significantly higher flexibility (evidenced by lower compressive force, *Figure 2A*) and comparable radial strength when compared with the metallic Xience DES (*Figure 2B*). The comparable radial strength of BVS with other metallic DES was attributed to the polymer processing technique (25).

In an independent bench study conducted by Ormiston *et al.*, a comparison was done between a metallic DES (ML8/Xpedition) and two PLLA-based BRS (Absorb BVS and Elixir's DESolve). A description of the three devices tested in this study can be seen in *Table 2*. It was reported that the ML8/Xpedition DES exhibited higher radial strength than Absorb BVS with both devices demonstrating similar recoil properties. For the two PLLA-based BRS, BVS was found to have significantly higher radial strength than Elixir's DESolve but DESolve showed self-correction after initial recoil (*Figure 2C-D*). The metallic DES had significantly higher safety thresholds in various post-dilatation strategies as compared to the PLLA-based counterparts (28). The self-correcting property of the DESolve BRS is a differentiating feature of the device. DESolve has demonstrated an ability to offset any initial recoiling of the device within the first few hours after implantation as the unconstrained device expands toward its nominal diameter. The potential

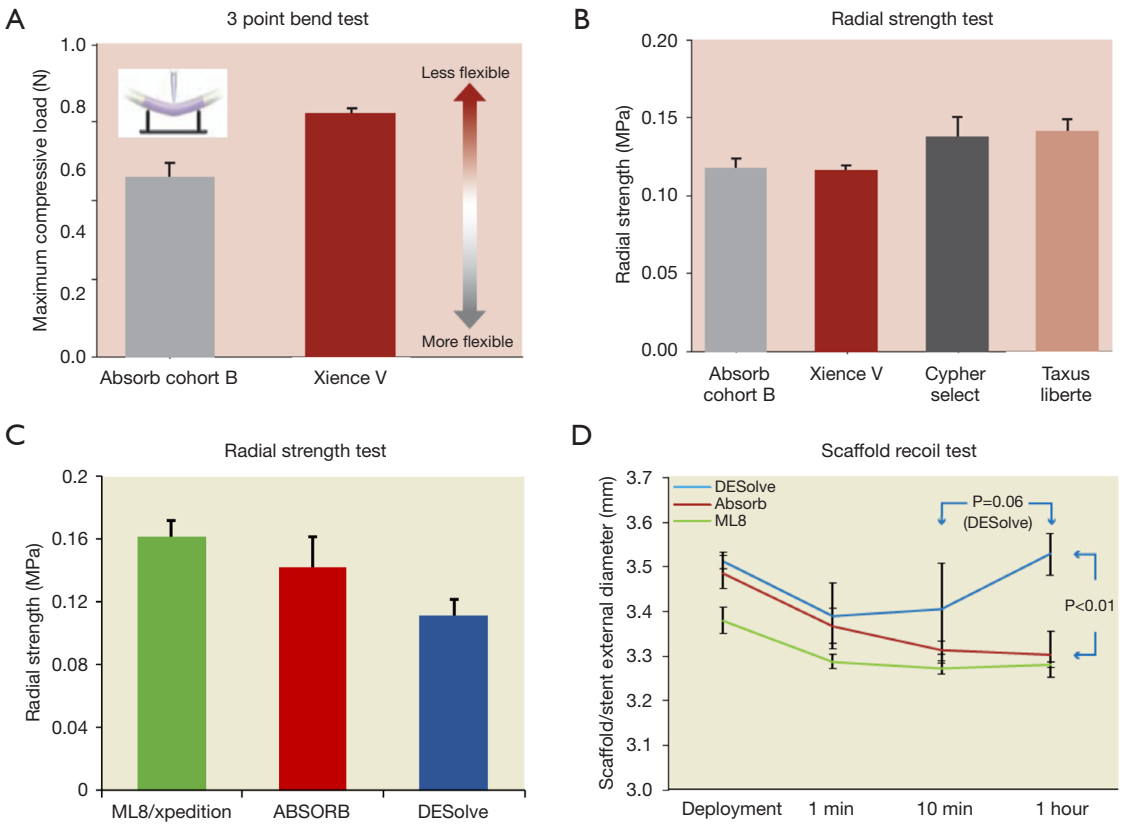

Figure 2 Mechanical properties of PLLA-based BRS and metallic DES measured using standard methods. (A) The data was based on maximum compressive load applied to deflect ABSORB cohort B and XIENCE V 3.0 mm × 18 mm devices by 1.1 mm; (B) the MSI RX550 radial expansion force gauge was employed to evaluate the acute radial strength data for the scaffolds/stents (n=5 for each set). Tests were performed by and data are on file at Abbott Vascular; (C) radial strength values (MPa) were plotted using the data from Mercy and Elixir testing; (D) scaffold/stent external difameter immediately after deployment, at 1, 10 min, then at 1 h. All figures are reprinted from EuroIntervention 5/F, Oberhauser *et al.*, *Design principles and performance of bioresorbable polymeric vascular scaffolds* (pF15-F22), Copyright (2009) and 11/1, Ormiston *et al.*, *An independent bench comparison of two bioresorbable drug-eluting coronary scaffolds (Absorb and DESolve) with a durable metallic drug-eluting stent (ML8/Xpedition)* (p60-67), Copyright [2015], with permission from Europa Digital & Publishing. BRS, bioresorbable scaffolds; DES, drug-eluting stents.

Table 2 A description of the devices used in an independent bench evaluation, adapted from (28)

BRS platform	ML8/Xpedition	Absorb BVS	DESolve
Manufacturer	Abbott Vascular	Abbott Vascular	Elixir Medical Corp
Backbone	Co-Cr	PLLA	PLLA-derived polymer
Coating	PVDF-HFP	PDLLA	PLA-based polymer
Peaks/hoop	6	6	9
Connections/hoop	3	3	3
Strut thickness (μm)	89	157	150
Drug	Everolimus	Everolimus	Novolimus

PVDF-HFP, poly(vinylidene fluoride-hexafluoropropylene).

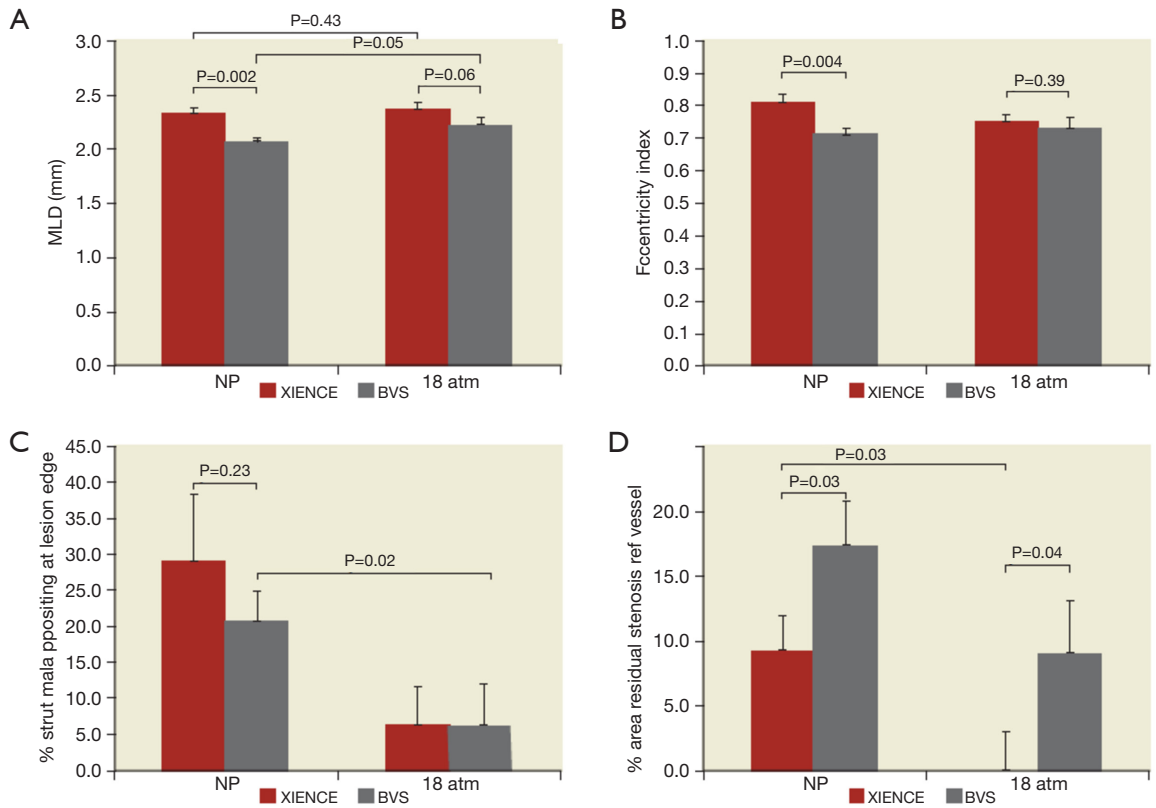

Figure 3 Results derived from OCT measurements in the *in-vitro* lesion models after deployment, representing. (A) MLD (minimal lumen diameter); (B) eccentricity index; (C) percentage strut malapposition at the lesion edge; and (D) percentage area residual stenosis of the BVS and Xience devices before (NP: nominal pressure) and after (18 atm) postdilatation. All figures are reprinted from EuroIntervention 12/7, Foin *et al.*, *Bioabsorbable Vascular Scaffold Radial Expansion and Conformation Compared to a Metallic platform: Insights from In-vitro Expansion in a Coronary Artery Lesion Model* (p834-844), Copyright [2016] with permission from Europa Digital & Publishing. BVS, bioresorbable vascular scaffold.

benefits of this self-correcting property include increasing scaffold dimensions, addressing the issue of scaffold under-deployment and reducing malapposition. This is especially useful in ST-segment elevation myocardial infarction (STEMI), in which infarct-related vessel dimensions have a tendency to increase over time after PCI (29,30).

In order to understand the mechanical performance of BVS in a more realistic setting, the expansion and conformation of BVS in an *in-vitro* lesion model was examined by Foin *et al.* (31). The constraining *in vitro* model was designed to reflect a lesion with 40% diameter stenosis and the results revealed that minimal lumen diameter (MLD) was significantly smaller while stent eccentricity was more marked in the BVS arm compared to Xience. These observations can be attributed to the difference in design and mechanical response between metallic stents and polymeric BRS (32,33). The study also revealed that performing post-dilatation after BVS implantation resulted in significant improvement in MLD, eccentricity and strut apposition (*Figure 3*). This emphasized the importance of lesion preparation, right sizing and post-dilatation in achieving optimal expansion of the BVS (31).

Vasomotion after BRS implantation

The vasomotion of the scaffolded/stented vessels between the BVS and Xience DES (*Figure 4A,B*) was examined in a preclinical porcine model. The results showed that vessels with the BVS demonstrated significantly restored in-scaffold vasomotor function at 1 and 2 years follow-up (34). Similarly, Elixir's DESolve BRS reported an increase in the scaffold area between 3 and 6 months. The scaffolded segments also displayed vasoreactivity similar to distal control, non-scaffolded segments, illustrating the

restoration of vascular tone (30).

Clinical observations

Acute procedural outcomes

The ABSORB II trial and other ABSORB studies share the same sentiments in terms of acute procedural outcomes between BVS and Xience devices. The angiographic outcome in the ABSORB II (501 patients) showed a difference in acute gain (MLA: 3.46 *vs*. 4.27 mm^2 for BVS and Xience respectively, P<0.001) although lesions' characteristics were similar in both groups. The differences in the inherent mechanical properties of PLLA (lower tensile and radial strength) were thought to have affected the robustness of the device during expansion. This outcome suggests that a more aggressive strategy during implantation and post-dilation of BVS as compared to metallic DES may be necessary (35). Other randomized controlled trials examining BVS and Xience have also reported a marked difference in procedural outcomes between both devices post-implantation. Results in terms of in-device acute gain, MLD were consistently lower in the BVS arm compared to the metallic Xience, with a significantly higher percentage diameter stenosis (*Table 3*) (36-39).

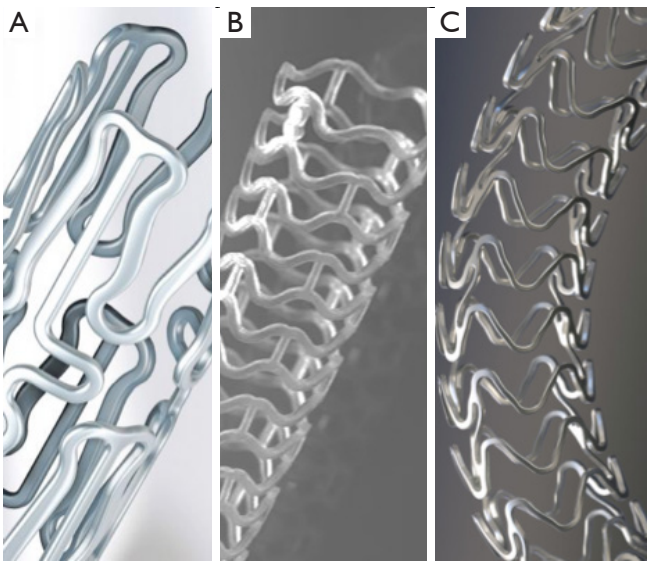

Figure 4 Images of Abbott Vascular's DES and BVS and Biotronik's BRS. (A) Abbott's cobalt-chromium Xience V DES; (B) Abbott's poly-L-lactic acid ABSORB BVS; (C) Biotronik magnesium alloy-based Magmaris BRS (images obtained from Abbott Vascular and Biotronik Inc. company websites).

Expansion, asymmetry and eccentricity

While analyzing acute procedural outcomes as indicators has been widely practiced, post-implantation device asymmetry and eccentricity is also important in examining optimal scaffold/stent expansion. Suwannasom *et al.* reported that optimal stent expansion was achieved in 20% of patients who received the Xience stent compared to 8% of those treated with Absorb BVS in the ABSORB II trial. Asymmetric expansion of the BVS was also associated with a nine-fold higher risk of adverse clinical outcomes (40). In another study, Dalos *et al.* investigated the device expansion uniformity of BVS and Xience (41). The extent of device expansion uniformity was measured by stent eccentricity index (SEI) and stent symmetry index (SSI) as defined by the following equations:

$$SEI=\frac{\text{Minimal scaffold/stent diameter}}{\text{Maximal scaffold/stent diameter}}$$

$$SSI=\frac{\text{Max.scaffold/stent diameter-Min.scaffold/stent diameter}}{\text{Max.scaffold/stent diameter}}$$

The results showed that BVS exhibited significantly lower SEI but higher SSI value than Xience, highlighting decreased uniformity in device expansion for the BVS. Local radial expansion was also found to be significantly reduced in BVS if no post-dilatation was employed (41). This lower

Table 3 Post-procedural in-device outcomes between the BVS and Xience across the ABSORB RCTs, adapted from (36-38)

Variables	ABSORB III		ABSORB China		ABSORB Japan	
	BVS	Xience	BVS	Xience	BVS	Xience
Total No. of patients	1,322	686	238	237	266	134
Post-dilatation performed, %	65.5	51.2	63	54.4	82.2	77.4
In-device acute gain (mm)	1.45±0.45	1.59±0.44	1.51±0.03	1.59±0.03	2.42±0.38	2.64±0.40
In-device MLD (mm)	2.37±0.40	2.49±0.40	2.48±0.02	2.59±0.03	1.46±0.40	1.65±0.40
In-device, diameter stenosis, %	11.6±88	6.4±8.9	12.2±0.47	8.7±0.46	11.8±7.4	7.1±8.0

MLD, minimal lumen diameter; BVS, bioresorbable vascular scaffold.

Table 4 Mechanical properties and *in vitro* degradation rate of different Mg alloys, adapted from (46-50)

Material	Metallurgy	Young's modulus (GPa)	Yield strength (MPa)	Tensile strength (MPa)	Elongation (%)	*In vitro* degradation, rate (mmy-1)
316L stainless steel	Annealed	193	190	490	40	Biostable
Pure Mg	As cast	41	20	86	13	407
AM60B-F	Die cast	45	–	220	6–8	8.97
WE43 alloy	Extruded	44	195	280	2	1.35
AZ31	Extruded	45	125–135	235	7	1.17
ZW21	Extruded	–	200	270	17	–
WZ21	Extruded	–	140	250	20	–
Mg-Zn	Extruded	42	170	280	19	0.16

The improved mechanical strength of the Mg alloys allows the resultant BRS to have potentially a higher radial strength for dilating atherosclerotic narrowing and thus higher acute gain of the coronary lumen (9,16). The theoretically higher radial strength also allows for thinner strut design as compared to polymer-based scaffolds, potentially improving the profile and deliverability of the BRS (9,16,17).

device expansion may potentially lead to an altered blood flow dynamics which can subsequently present as a source for acute and subacute post-procedural issues (42). In another study, Mattesini *et al.* found no difference in stent eccentricity when aggressive lesion preparation and post dilatation were used for BVS implantation. These results demonstrated the key role lesion preparation plays in the optimal/maximal expansion of the BVS, particularly in the presence of calcified/stiff fibrous lesions (31,43,44). Recent clinical data has also highlighted the importance of implantation procedure on clinical outcomes of the BVS and improvement was observed in the pooled ABSORB trials outcome when BVS specific strategy is adopted (45).

Metallic-based BRS

Bio-corrodible or biodegradable metallic stents sought to combine the benefits of using a transient scaffold with stronger mechanical properties of metals as compared to polymer-based BRS. Mg is a suitable candidate due to its relatively low corrosion resistance and biocompatibility of the metal and the corrosion reaction products. However, Mg implants are known to degrade quickly in aggressive chloride environments like body fluid, resulting in rapid accumulation of degradation products at the tissue which can cause neointimal formation. This accelerated degradation will also lead to a decrease in device integrity, thereby limiting its use as a medical implant material. Hence, Mg is often alloyed with other elements such as aluminum and manganese to retard its degradation rate (46). The mechanical properties and *in vitro* degradation rate of some of the Mg alloys are summarized in *Table 4*.

Mechanical properties of metallic-based BRS

Bioresorption of Mg

The degradation of Mg implants is expected to undergo these two steps:

(I) Conversion of Mg alloy to hydrated Mg oxide (corrosion reaction with water) (16,51),
$Mg\ (s) + 2H_2O\ (aq) \rightarrow Mg\ (OH)_2\ (s) + H_2\ (g)$

(II) Conversion of Mg oxide to Mg phosphate and subsequent replacement by amorphous calcium phosphate. Mg is removed by diffusion from the amorphous matrix and is absorbed by the body (52).

The rapid degradation rate of Mg alloys due to poor corrosion resistance property limits the use of the material in implantable biomedical devices. The formation of hydrogen during corrosion and a shift in the alkaline pH near the corroding surface are of concerns for medical applications. There are two possible methods to improve the corrosion behavior of Mg alloys:

(I) Design the composition and microstructure (e.g., grain size, texture) of the base material through optimized processing methods.

(II) Apply surface treatment on the Mg alloy to form protective coatings (e.g., ceramic, polymeric or composite layers) (53).

One effective method to improve the corrosion resistance is the use of a polymeric coating to tailor the degradation

rate of the Mg material, while also serving as a drug coating. Biodegradable polymers such as polyglycolide, polylactide and PCL have been examined as potential coating for Mg alloys due to their good biocompatibility lower degradation rates than Mg materials. A study conducted by Xu *et al.* revealed that Mg coated with high molecular weight PLLA displayed a significantly lower corrosion rate compared to uncoated Mg (54). Other polymers such as PCL has also been investigated as protective coating and to improve corrosion resistance and cytocompatibility of Mg implants (55). Metallic-based BRS such as drug eluting absorbable magnesium scaffolds (DREAMS), also known as the Magmaris, from Biotronik and the BIOLUTE BRS (Envision Scientific) employ Mg alloy as the stent material.

Magmaris BRS

The DREAMS series stent (Biotronik, Berlin, Germany) was redesigned from its predecessor absorbable Mg scaffold (AMS) with the following improvements (16,56):

(I) A Mg alloy with a higher collapse pressure and slower resorption.
(II) Change in cross-sectional shape from rectangular to square struts.
(III) Reduced strut thickness.
(IV) Inclusion of an anti-proliferative drug-eluting polymeric coating.

A polymeric coating was also added to the DREAMS BRS to further decrease the degradation rate, while releasing 1.4 μg/mm^2 of sirolimus. The 2nd generation DREAMS stent (DREAMS 2G/Magmaris) (*Figure 4C*) has a sirolimus coating and an improved 6-crown 2-link design which provided greater radial stiffness and mechanical strength. The device received its CE mark approval in 2016. It has been reported that the radial stiffness the Magmaris BRS at 1.38 N/mm is comparable to conventional durable metal stents (17). The recently presented BIOSOLVE II trial was a prospective, multicenter trial that enrolled 123 patients to evaluate the Magmaris stent. The study revealed no definite or probable scaffold thrombosis or any additional clinically driven target vessel revascularization at 6 months. The clinical outcomes showed improved results of the device compared with its predecessors while preserving an agreeable clinical and safety profile (52).

Polymer-based vs. metallic-based BRS

In vitro observations

An *in vitro* bench test study conducted by Schmidt *et al.* compared the mechanical performance of the Absorb BVS (PLLA), DESolve (PLLA) and Magmaris (Mg) BRS. The study reported that the Magmaris had the lowest recoil after implantation (acute and after 1 h), followed by the BVS and lastly DESolve in a mock vessel model. This showed that time-dependent recoil occurred consistently in the polymer-based BRS but not for Magmaris, where the mechanical behavior remained constant after expansion and over time (57).

The deliverability of the three BRS was also measured based on the track force (trackability) measured where low forces represent easy access. The best trackability was found to be the DESolve, followed by the Magmaris and Absorb BVS. The bending stiffness of the Magmaris was found to be lower than the BVS in both the crimped and expanded state, suggesting better vessel conformity. The radial strength (measured in terms of collapse pressure of the device) of Magmaris was significantly higher than that of the BVS (57).

Preclinical/clinical observations

In a recent study published by Waksman *et al.*, the safety and efficacy of the Magmaris was compared with Absorb BVS and Xience in porcine and rabbit models. It was reported that the Magmaris displayed a higher endothelialization rate after 28 days compared to the BVS. Between Magmaris and Xience, vascular compatibility (neoinitmal growth, inflammation, fibrin deposition) was found to be similar up to 2 years follow-up. The Magmaris also exhibited moderate late lumen loss at 180 days but showed late lumen gain at 2 years, suggesting potential vascular restoration (58). However, Koppara *et al.* showed that this preclinical data affirmed the efficacy and safety profile of the Magmaris compared to BVS and Xience which are currently in clinical use.

Angiographic and imaging data obtained from recent clinical studies suggested different acute expansion outcomes and resorption behavior from the three devices. *Table 5* is a comparison of stent specifications and 1-year clinical outcomes between the metallic Xience, PLLA BVS and the Magmaris (59). Post-procedural MLD was largest in Xience (2.53±0.40 mm), followed by Magmaris (2.46±0.33 mm) and then the BVS (2.37±0.39 mm). Xience also obtained the larger in-device acute gain compared to the BVS and Magmaris (39). QCA data revealed that high late loss was observed in the Magmaris at 6 months follow-up, which remained the case at the end of 12 months (37). The loss in minimum lumen area at 6 months in the Magmaris was attributed to a reduction in the minimum scaffold area rather

Table 5 Comparison of stent specifications and 1-year clinical outcome between Co-Cr Xience, PLLA Absorb BVS and Mg Magmaris. Adapted from (59)

Platform	Xience	Absorb BVS	Magmaris
Core material	Co-Cr	PLLA	Refined Mg alloy
Strut thickness/width	89/89–112 μm	157/191 μm	150/150 μm, (ø 3.0&3.5)
Strut to artery ratio (%)	13	27	20
Absorption time	N/A	~24 months	~12 months
Device clinical results (%)			
Composite TLF	5.2	6.6	3.4
Cardiac death	0.3	0.4	0.8
Target vessel MI	3.3	5.1	0.8
TLR	2.3	2.7	1.7
Device thrombosis	0.6	1.3	0
Device angiographic results (mm)			
Pre-procedural MLD	0.95 (0.36)	0.96 (0.37)	1.22 (0.33)
Post-procedural MLD	2.53 (0.40)	2.37 (0.39)	2.54 (0.33)
Follow-up MLD	2.50 (0.03)	2.27 (0.03)	2.10 (0.41)
In device acute gain	1.58 (0.43)	1.41 (0.45)	1.29 (0.34)
In device late loss	0.10 (0.02)	0.23 (0.03)	0.39 (0.27)

Strut to artery ratio (SAR) in percentage for 3.0 mm device expanded at nominal diameter. Target vessel myocardial infarction (MI). Values are represented in mean (SD). MLD, acute gain and late loss data of Xience and BVS were obtained from (37,60) and the Magmaris data was obtained from (52). TLR, target lesion revascularization. Table reprinted from International Journal of Cardiology 223, Foin *et al*., Current bioresorbable scaffold technologies for treatment of coronary artery diseases: Do polymer and Magnesium platforms differ? (p526-528), Copyright [2016] with permission from Elsevier Inc.

than neointimal hyperplasia (52). It remains to be seen if positive vessel remodeling can make up for this early lumen loss though early clinical results suggest that clinical outcomes and target vessel revascularization were not affected.

Updated clinical data

Abbott's BVS short-term clinical efficacy (at 1-year follow-up) has comparable outcomes as the metallic Xience but the proposed long term benefits remain to be seen. Clinical outcomes from the AIDA (Amsterdam Investigator-Initiated Absorb Strategy All-Comers) trial has also affirmed the significant increased risk of scaffold thrombosis in patients receiving the BVS compared to those with Xience. Although there was no significant difference in the risk of target-vessel or target-lesion failure among patients, it was observed that a higher risk of scaffold thrombosis was evident in the subacute phase as well as late and very late phases in the BVS arm (61).

The recent 3-year follow-up from the ABSORB II trial reported that vasomotor reactivity was not statistically different between the two devices while late lumen loss was significantly larger in the BVS arm. The BVS group also recorded eight definite scaffold thromboses and one late probable scaffold thrombosis and no definite or probable stent thrombosis in Xience (62). Two-year follow-up results from the ABSORB III trial on the other hand, revealed an increase in major adverse cardiac events for BVS compared to Xience group (TLF: 11.0% *vs.* 7.9%, P=0.03; target-vessel MI: 7.3% *vs.* 4.9%, P=0.04) (63). This outcome has prompted the FDA to investigate the increased 2-year MACE observed with the BVS. EU regulatory authority and Abbott Vascular have also decided to restrict commercial availability of the device in Europe from May 2017 onwards.

Conclusions

The *in vitro* and *in vivo* observations of the polymer and metallic-based scaffolds have highlighted the distinct material properties and performance of the two BRS platforms. This has led to different behavior of the devices in terms of expansion, elastic and time-dependent recoil as well as radial strength. It has been suggested that the time dependent behavior is typical for polymer-based BRS while the metallic Mg stent displayed quick expansion and stable acute mechanics. Presently, both the polymer-based and Mg-based BRS platforms remain limited by their large profile and strut thickness, as compared to metallic DES. Clinical outcomes from recent trials revealed that second generation DES are still performing better than the BRS in terms of post procedural acute gain, minimizing early late lumen loss and stent thrombosis. The expectation is that the BVS and Magmaris can undergo bioresorption and allow the lumen to evolve and remodel positively (64). Longer-term data from the ABSORB III and IV program will reveal whether better patient selection and technique improves the short outcomes, and if the BVS improves late outcomes compared to Xience. More trials examining the performance and clinical outcomes of the Magmaris BRS at later time points are required to deepen our understanding on the difference in lumen dynamics between the polymer and metallic-based platforms.

Acknowledgements

None.

Footnote

Conflicts of Interest: The authors have no conflicts of interest to declare.

References

1. Stefanini GG, Taniwaki M, Windecker S. Coronary stents: novel developments. Heart 2014;100:1051-61.
2. Gonzalo N, Macaya C. Absorbable stent: focus on clinical applications and benefits. Vasc Health Risk Manag 2012;8:125-32.
3. Wiebe J, Nef HM, Hamm CW. Current status of bioresorbable scaffolds in the treatment of coronary artery disease. J Am Coll Cardiol 2014;64:2541-51.
4. Takayama T, Hiro T, Hirayama A. Stent thrombosis and drug-eluting stents. Journal of Cardiology 2011;58:92-8.
5. Kawaguchi R, Angiolillo DJ, Futamatsu H, et al. Stent thrombosis in the era of drug eluting stents. Minerva Cardioangiol 2007;55:199-211.
6. Joner M, Finn AV, Farb A, et al. Pathology of drug-eluting stents in humans: delayed healing and late thrombotic risk. J Am Coll Cardiol 2006;48:193-202.
7. Natsuaki M, Morimoto T, Furukawa Y, et al. Late adverse events after implantation of sirolimus-eluting stent and bare-metal stent: long-term (5-7 years) follow-up of the Coronary Revascularization Demonstrating Outcome study-Kyoto registry Cohort-2. Circ Cardiovasc Interv 2014;7:168-79.
8. Sharkawi T, Cornhill F, Lafont A, et al. Intravascular bioresorbable polymeric stents: a potential alternative to current drug eluting metal stents. J Pharm Sci 2007;96:2829-37.
9. Ielasi A, Tespili M. Current Status and Future Perspectives on Drug-eluting Bioresorbable Coronary Scaffolds: Will the Paradigm of PCI Shfit? EMJ Int Cardiol 2014;1:81-90.
10. Garg S, Serruys PW. Coronary stents: looking forward. J Am Coll Cardiol 2010;56:S43-78.
11. Neamtu I, Chiriac AP, Diaconu A, et al. Current concepts on cardiovascular stent devices. Mini Rev Med Chem 2014;14:505-36.
12. Pinto Slottow TL, Waksman R. Overview of the 2006 Food and Drug Administration Circulatory System Devices Panel meeting on drug-eluting stent thrombosis. Catheter Cardiovasc Interv 2007;69:1064-74.
13. Iqbal J, Onuma Y, Ormiston J, et al. Bioresorbable scaffolds: rationale, current status, challenges, and future. Eur Heart J 2014;35:765-76.
14. Kohn J, Zeltinger J. Degradable, drug-eluting stents: a new frontier for the treatment of coronary artery disease. Expert Rev Med Devices 2005;2:667-71.
15. Berglund J, Guo Y, Wilcox JN. Challenges related to development of bioabsorbable vascular stents. EuroIntervention 2009;5 Suppl F:F72-9.
16. Campos CM, Muramatsu T, Iqbal J, et al. Bioresorbable drug-eluting magnesium-alloy scaffold for treatment of coronary artery disease. Int J Mol Sci 2013;14:24492-500.
17. Alexy RD, Levi DS. Materials and manufacturing technologies available for production of a pediatric bioabsorbable stent. Biomed Res Int 2013;2013:137985.
18. Ang HY, Bulluck H, Wong P, et al. Bioresorbable stents: Current and upcoming bioresorbable technologies. Int J Cardiol 2017;228:931-9.
19. Onuma Y, Ormiston J, Serruys PW. Bioresorbable scaffold

technologies. Circ J 2011;75:509-20.
20. Garcia-Garcia HM, Serruys PW, Campos CM, et al. Assessing bioresorbable coronary devices: methods and parameters. JACC Cardiovasc Imaging 2014;7:1130-48.
21. Makadia HK, Siegel SJ. Poly Lactic-co-Glycolic Acid (PLGA) as Biodegradable Controlled Drug Delivery Carrier. Polymers 2011;3:1377-97.
22. Vroman I, Tighzert L. Biodegradable Polymers. Materials 2009;2:307-44.
23. Kwon DY, Kim JI, Da YK, et al. Biodegradable stent. J Biomed Sci Eng 2012;5:208-16.
24. Ormiston JA, De Vroey F, Serruys PW, et al. Bioresorbable polymeric vascular scaffolds: a cautionary tale. Circ Cardiovasc Interv 2011;4:535-8.
25. Oberhauser JP, Hossainy S, Rapoza RJ. Design principles and performance of bioresorbable polymeric vascular scaffolds. EuroIntervention 2009;5 Suppl F:F15-22.
26. Gajjar RC, King WM. Resorbable Fiber-Forming Polymers for Biotextile Applications. SpringerBriefs in Materials: Springer International Publishing, 2014:(7-10).
27. Onuma Y, Serruys PW. Bioresorbable Scaffold: The Advent of a New Era in Percutaneous Coronary and Peripheral Revascularization? Circulation 2011;123:779-97.
28. Ormiston JA, Webber B, Ubod B, et al. An independent bench comparison of two bioresorbable drug-eluting coronary scaffolds (Absorb and DESolve) with a durable metallic drug-eluting stent (ML8/Xpedition). EuroIntervention 2015;11:60-7.
29. Verheye S, Ormiston JA, Stewart J, et al. A Next-Generation Bioresorbable Coronary Scaffold System: From Bench to First Clinical Evaluation: 6- and 12-Month Clinical and Multimodality Imaging Results. JACC Cardiovasc Interv 2014;7:89-99.
30. Nef HM, Wiebe J, Foin N, et al. A new novolimus-eluting bioresorbable coronary scaffold: Present status and future clinical perspectives. Int J Cardiol 2017;227:127-33.
31. Foin N, Lee R, Bourantas C, et al. Bioresorbable vascular scaffold radial expansion and conformation compared to a metallic platform: insights from in vitro expansion in a coronary artery lesion model. EuroIntervention 2016;12:834-44.
32. Foin N, Lee RD, Torii R, et al. Impact of stent strut design in metallic stents and biodegradable scaffolds. Int J Cardiol 2014;177:800-8.
33. Bourantas CV, Onuma Y, Farooq V, et al. Bioresorbable scaffolds: Current knowledge, potentialities and limitations experienced during their first clinical applications. Int J Cardiol 2013;167:11-21.
34. Gogas BD, Benham JJ, Hsu S, et al. Vasomotor Function Comparative Assessment at 1 and 2 Years Following Implantation of the Absorb Everolimus-Eluting Bioresorbable Vascular Scaffold and the Xience V Everolimus-Eluting Metallic Stent in Porcine Coronary Arteries. Insights From In Vivo Angiography, Ex Vivo Assessment, and Gene Analysis at the Stented/Scaffolded Segments and the Proximal and Distal Edges. JACC Cardiovasc Interv 2016;9:728-41.
35. Sotomi Y, Ishibashi Y, Suwannasom P, et al. Acute Gain in Minimal Lumen Area Following Implantation of Everolimus-Eluting ABSORB Biodegradable Vascular Scaffolds or Xience Metallic StentsIntravascular Ultrasound Assessment From the ABSORB II Trial. JACC Cardiovasc Interv 2016;9:1216-27.
36. Ellis SG, Kereiakes DJ, Metzger DC, et al. Everolimus-Eluting Bioresorbable Scaffolds for Coronary Artery Disease. New Engl J Med 2015;373:1905-15.
37. Gao R, Yang Y, Han Y, et al. Bioresorbable Vascular Scaffolds Versus Metallic Stents in Patients With Coronary Artery DiseaseABSORB China Trial. J Am Coll Cardiol 2015;66:2298-309.
38. Kimura T, Kozuma K, Tanabe K, et al. A randomized trial evaluating everolimus-eluting Absorb bioresorbable scaffolds vs. everolimus-eluting metallic stents in patients with coronary artery disease: ABSORB Japan. Eur Heart J 2015;36:3332-42.
39. Serruys PW, Chevalier B, Dudek D, et al. A bioresorbable everolimus-eluting scaffold versus a metallic everolimus-eluting stent for ischaemic heart disease caused by de-novo native coronary artery lesions (ABSORB II): an interim 1-year analysis of clinical and procedural secondary outcomes from a randomised controlled trial. Lancet 2015;385:43-54.
40. Suwannasom P, Sotomi Y, Ishibashi Y, et al. The Impact of Post-Procedural Asymmetry, Expansion, and Eccentricity of Bioresorbable Everolimus-Eluting Scaffold and Metallic Everolimus-Eluting Stent on Clinical Outcomes in the ABSORB II Trial. JACC Cardiovasc Interv 2016;9:1231-42.
41. Dalos D, Gangl C, Roth C, et al. Mechanical properties of the everolimus-eluting bioresorbable vascular scaffold compared to the metallic everolimus-eluting stent. BMC Cardiovasc Disord 2016;16:104.
42. Otake H, Shite J, Ako J, et al. Local determinants of thrombus formation following sirolimus-eluting stent implantation assessed by optical coherence tomography. JACC Cardiovasc Interv 2009;2:459-66.

43. Panoulas VF, Miyazaki T, Sato K, et al. Procedural outcomes of patients with calcified lesions treated with bioresorbable vascular scaffolds. EuroIntervention 2016;11:1355-62.
44. Mattesini A, Secco GG, Dall'Ara G, et al. ABSORB biodegradable stents versus second-generation metal stents: a comparison study of 100 complex lesions treated under OCT guidance. JACC Cardiovasc Interv 2014;7:741-50.
45. Rizik DG, Hermiller JB, Kereiakes DJ. The ABSORB bioresorbable vascular scaffold: A novel, fully resorbable drug-eluting stent: Current concepts and overview of clinical evidence. Catheter Cardiovasc Interv 2015;86:664-77.
46. Moravej M, Mantovani D. Biodegradable Metals for Cardiovascular Stent Application: Interests and New Opportunities. Int J Mol Sci 2011;12:4250-70.
47. Hermawan H, Moravej M, Dubé D, et al. Degradation Behaviour of Metallic Biomaterials for Degradable Stents. Adv Mater Res 2007;15-7:113-8.
48. Gu XN, Zheng YF. A review on magnesium alloys as biodegradable materials. Front Mater Sci China 2010;4:111-5.
49. Lévesque J, Hermawan H, Dubé D, et al. Design of a pseudo-physiological test bench specific to the development of biodegradable metallic biomaterials. Acta Biomater 2008;4:284-95.
50. Bowen PK, Shearier ER, Zhao S, et al. Biodegradable Metals for Cardiovascular Stents: from Clinical Concerns to Recent Zn-Alloys. Adv Healthc Mater 2016;5:1121-40.
51. Shi YJ, Pei J, Zhang J, et al. Enhanced corrosion resistance and cytocompatibility of biodegradable Mg alloys by introduction of Mg(OH)2 particles into poly (L-lactic acid) coating. Sci Rep 2017;7:41796.
52. Haude M, Ince H, Abizaid A, et al. Safety and performance of the second-generation drug-eluting absorbable metal scaffold in patients with de-novo coronary artery lesions (BIOSOLVE-II): 6 month results of a prospective, multicentre, non-randomised, first-in-man trial. Lancet 2016;387:31-9.
53. Hornberger H, Virtanen S, Boccaccini AR. Biomedical coatings on magnesium alloys – A review. Acta Biomaterialia 2012;8:2442-55.
54. Xu L, Yamamoto A. In vitro degradation of biodegradable polymer-coated magnesium under cell culture condition. Appl Surf Sci 2012;258:6353-8.
55. Xu L, Yamamoto A. Characteristics and cytocompatibility of biodegradable polymer film on magnesium by spin coating. Colloids Surf B Biointerfaces 2012;93:67-74.
56. Muramatsu T, Onuma Y, Zhang YJ, et al. Progress in treatment by percutaneous c oronary intervention: the stent of the future. Rev Esp Cardiol (Engl Ed) 2013;66:483-96.
57. Schmidt W, Behrens P, Brandt-Wunderlich C, et al. In vitro performance investigation of bioresorbable scaffolds - Standard tests for vascular stents and beyond. Cardiovasc Revasc Med 2016;17:375-83.
58. Waksman R, Zumstein P, Pritsch M, et al. Second-generation Magnesium Scaffold Magmaris, Device Design, and Preclinical Evaluation in a Porcine Coronary Artery Model. EuroIntervention 2017;13:440-449.
59. Foin N, Ng J, Wong P, et al. Current bioresorbable scaffold technologies for treatment of coronary artery diseases: Do polymer and Magnesium platforms differ? Int J Cardiol 2016;223:526-8.
60. Stone GW, Gao R, Kimura T, et al. 1-year outcomes with the Absorb bioresorbable scaffold in patients with coronary artery disease: a patient-level, pooled meta-analysis. Lancet 2016;387:1277-89.
61. Wykrzykowska JJ, Kraak RP, Hofma SH, et al. Bioresorbable Scaffolds versus Metallic Stents in Routine PCI. N Engl J Med 2017;376:2319-28.
62. Serruys PW, Chevalier B, Sotomi Y, et al. Comparison of an everolimus-eluting bioresorbable scaffold with an everolimus-eluting metallic stent for the treatment of coronary artery stenosis (ABSORB II): a 3 year, randomised, controlled, single-blind, multicentre clinical trial. Lancet 2016;388:2479-91.
63. Ellis SG, Kereiakes DJ, Stone GW. Everolimus-eluting Bioresorbable Vascular Scaffolds in Patients with Coronary Artery Disease: ABSORB III Trial 2-Year Results. Presented at The ACC, 2017; Florida, USA.
64. Serruys PW, Onuma Y, Garcia-Garcia HM, et al. Dynamics of vessel wall changes following the implantation of the absorb everolimus-eluting bioresorbable vascular scaffold: a multi-imaging modality study at 6, 12, 24 and 36 months. EuroIntervention 2014;9:1271-84.

Cite this article as: Ang HY, Huang YY, Lim ST, Wong P, Joner M, Foin N. Mechanical behavior of polymer-based *vs*. metallic-based bioresorbable stents. J Thorac Dis 2017;9(Suppl 9):S923-S934. doi: 10.21037/jtd.2017.06.30

